

On the design of PARACEST agents for clinical applications: SAR considerations

I. Hancu¹, T. W. Dixon¹, R. E. Lenkinski², A. D. Sherry³, D. E. Woessner³

¹GE GRC, Niskayuna, NY, United States, ²Harvard Med. School, Boston, MA, United States, ³Univ. of Texas Southwestern Med. Ctr., Dallas, TX, United States

Introduction

Paramagnetic Chemical Exchange Saturation Transfer (PARACEST) agents have recently emerged as a new class of MRI contrast agents [1]. Their enticing advantages include the ability to be switched on or off at will and their capability to report quantitatively on their surrounding environment (eg pH [2]). Two issues must be addressed through careful design for this novel concept to reach the clinic: toxicity must be low, and the desired contrast has to be obtained through RF irradiation compliant with FDA specific absorption rate (SAR) guidelines. Here we present a model that gives insight into ways to optimize the PARACEST agents to offer maximum contrast while irradiated with a B_1 compliant with the FDA guidelines.

Methods

The contrast given by a typical PARACEST agent [1] was modeled using the Bloch equations for 3 spin pools, coupled through chemical exchange [3]. The free water pool was exchanging with the water molecules transiently bound to the agent, as well as with the amide protons on the chelator. Due to steric considerations, no exchange was assumed between the bound water and the amide protons. Theoretical predictions were validated on a phantom containing 62.5mM of an Eu^{3+} complex of a DOTA tetra(amide) derivative (1,4,7,10 tetraazacyclododecane tetrakis (ethyl-acetamidoacetate))- referred to as agent **1** [1]. Experiments were performed on a 1.5T clinical scanner, using a custom-built birdcage coil (12cm diameter, 16cm length). All measurements (including z-spectra- ie saturation as a function of frequency offset) were done on an imaging basis, using a GRE sequence (TE/TR=6/116ms), flip angle 15 degrees, which included a 60ms Fermi pulse for selective saturation of the bound water pool. Each image took 10 seconds to collect, and 61 images were acquired for a z-spectrum (ranging from -6000 to +6000Hz, in 200Hz steps). ROI's within the phantom containing the contrast agent were then selected in the magnitude images, and intensities recorded as a function of irradiation offset.

Results and discussion

Figure 1a and 1b present typical phantom images, irradiated at +3000Hz (at the frequency of the bound resonance), and symmetrically at -3000Hz, with a B_1 strength of 470Hz. A 40% signal decrease can be observed in the regions of the phantom containing the contrast agent (inner compartment), while no signal change is observed in the outer compartment, which only contains CuSO_4 doped water.

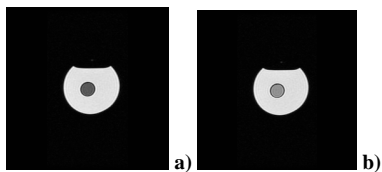


Figure1: Phantom image with pre-irradiation at a) +3000 and b) -3000Hz

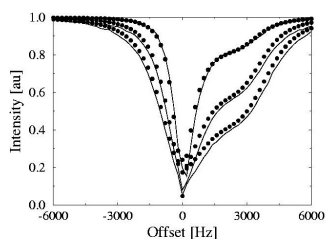


Figure2: Experimental data (circles) and theoretical prediction (solid lines) for the z-spectra of 62.5mM of agent **1**

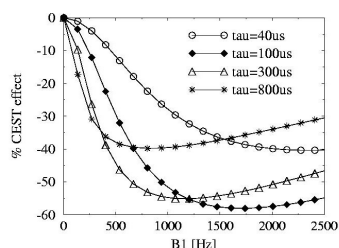


Figure3: Theoretical simulations for %CEST as a function of RF strength for various proton exchange lifetimes

Figure 2 presents experimental data (circles) from 3 z-spectra, acquired with 3 different irradiation strengths (264 Hz-inner-most curve, 500 Hz and 746 Hz- outer-most curve). The 8 parameters pertinent to the model (6 relaxation rates for the 3 pool model, plus two exchange rates) were adjusted to produce a good match between the experimental data for the lowest irradiation strength and the theoretical prediction (solid line). All the parameters were then kept constant, and the theoretical curves for the higher irradiation strengths were generated. Good qualitative agreement can be noticed between the theoretical predictions and experimental data, indicating that the model is appropriate for describing the contrast obtained as a function of agent characteristics and applied RF field.

Figure 3 presents the theoretical contrast as a function of B_1 obtained for hypothetical CEST agents having exactly the same characteristics as the above agent, EXCEPT for the exchange lifetime for the bound water protons, which took the values of 40, 100, 300 and 800 μs . All other acquisition parameters were kept constant for the 4 agents. The % contrast has been defined with respect to control irradiation, therefore at high B_1 's a decrease in the % contrast due to "leak-through" saturation of the free water pool can be seen. It has long been known that, with no SAR limit, the agents with the shortest proton lifetime (but still in slow exchange $\tau \cdot \Delta\omega \gg 1$) produce the most contrast. As one can notice from Figure 3, though, given a maximum irradiation strength which is tolerable from the SAR perspective, there is an optimum exchange lifetime that produces the maximum %contrast for a given agent concentration. In particular, for a head scan of a 200lb person at 1.5T, a B_1 on the order of 325Hz will be tolerable from the SAR perspective (given the acquisition parameters mentioned above), leading to an optimum proton exchange lifetime of $\sim 500\mu\text{s}$ (the optimum lifetime can be expressed as $1/\tau = 2\pi B_1$). Once the agent characteristics are known, the agent concentration needed for observing a minimum effect (eg 5%) can be easily calculated.

Conclusions

A theory has been presented to link the contrast obtained with PARACEST agents to their physical characteristics (relaxation times and exchange lifetimes) and to the applied saturating RF field. It has been determined that there is an optimum proton exchange lifetime for such agents to give maximum contrast when SAR guidelines are to be observed. This optimum lifetime is a function of application (body part to be studied), as the function which relates B_1 to SAR depends, among others, on sample geometry and tissue conductivity. The optimum bound proton lifetime is also a function of coil size and type (volume vs surface coil) and field strength. Increasing the number of exchangeable shifted protons per paramagnetic ion in a PARACEST contrast agent is very important to pursue, to observe detectable contrast at sub mM concentrations.

References

1. Zhang et al, JACS **123**, 1517 (2001);
2. Aime et al, Magn Res Med, **47**, 639 (2002);
3. Baguet et al, JMR **128**, 149 (1997);